Arch Toxicol (2014) 88:97–107
DOI 10.1007/s00204-013-1085-6

MOLECULAR TOXICOLOGY

V8, a newly synthetic flavonoid, induces apoptosis through ROS-mediated ER stress pathway in hepatocellular carcinoma

Yi Zhang · Li Zhao · Xin Li · Yajing Wang · Jing Yao · Hu Wang · Fanni Li · Zhiyu Li · Qinglong Guo

Received: 22 February 2013 / Accepted: 20 June 2013 / Published online: 9 July 2013

Abstract Natural flavonoids from plants have been demonstrated to possess promising chemopreventive activities against various diseases. 7-{4-[Bis-(2-hydroxy-ethyl)-amino]-butoxy}-5-hydroxy-8-methoxy-2-phenyl-chromen-4-one (V8), a newly synthesized derivative of wogonin may have antioxidant, antiviral, anti-inflammatory and anti-tumor potentials as wogonin. Based on the recent findings of V8, the anti-tumor activities and fundamental mechanisms by which V8 inhibits growth of hepatocellular carcinoma were further investigated in this study. After the treatment of V8, a significant inhibition of HepG2 cell proliferation was observed in a dose-dependent manner with the IC_{50} value of 23 μM using MTT assay. The exposure to V8 also resulted in apoptosis induction and an accumulation of ROS and Ca^{2+}. Meanwhile, a release of cytochrome c (Cyt-c), activation of BH-3 only proteins and Bax, decrease in mitochondrial membrane potential ΔΨ, as well as a suppression of Bcl-2, pro-caspase9 and pro-caspase3 expression were shown. Moreover, knocking down CHOP partly decreased the effect of V8-mediated apoptosis and activation of GRP78, p-PERK, p-eIF2α, ATF4 and CHOP modulated ER stress triggered by V8. In vivo, V8 inhibited the transplanted mice H22 liver carcinomas in a dose-dependent manner. Compared with wogonin, V8 exhibited stronger anti-proliferative effects both in vitro and in vivo. The underlying mechanism of activating PERK-eIF2α-ATF4 pathway by which V8 induces apoptosis was verified once again in vivo. The apoptosis induction via the mitochondrial pathway by modulating the ROS-mediated ER signaling pathway might serve to provide support for further studies of V8 as a possible anticancer drug in the clinical treatment of cancer.

Keywords V8 · Apoptosis · ER stress · ROS · Hepatocellular carcinoma

Abbreviations

ROS	Reactive oxygen species
ER	Endoplasmic reticulum
HCC	Hepatocellular carcinoma
UPR	Unfolded protein response
ΔΨm	Mitochondrial transmembrane potential
CHOP	CCAAT/enhancer-binding protein–homologous protein
DMSO	Dimethyl sulfoxide
NAC	N-acetyl cysteine
carboxy-H2DCFDA	Dichlorofluorescein diacetate
ERAD	ER-associated degradation

Introduction

Hepatocellular carcinoma (HCC) is a refractory malignancy with high incidence and mortality rates (El-Serag

Yi Zhang and Li Zhao have contributed equally to this article.

Y. Zhang · L. Zhao · X. Li · J. Yao · H. Wang · F. Li · Q. Guo (✉)
State Key Laboratory of Natural Medicines, Jiangsu Key Laboratory of Carcinogenesis and Intervention, China Pharmaceutical University, 24 Tongjiaxiang, Nanjing 210009, People's Republic of China
e-mail: anticancer_drug@163.com

Y. Wang
Department of Physiology, China Pharmaceutical University, 24 Tongjiaxiang, Nanjing 210009, People's Republic of China

Z. Li (✉)
School of Pharmacy, China Pharmaceutical University, Nanjing 210009, People's Republic of China
e-mail: zhiyuli@263.net

2011; Jemal et al. 2011). It is the most common primary hepatic tumor and the fifth most common tumor worldwide (Llovet et al. 2008; Motola-Kuba et al. 2006). Although a great achievement in HCC has been acquired during the past three decades, patients continue to experience a poor prognosis because of the lack of an effective systemic treatment regimen (Bruix and Llovet 2009; Whittaker et al. 2010). The current treatment modalities, including surgical resection and liver transplantation, cannot take a significant effect on HCC (Gish and Baron 2008; Ye 2008). Therefore, finding new targeted agents or combination chemotherapy is crucial to the treatment of hepatocellular carcinoma.

The endoplasmic reticulum (ER) is the intracellular organelle responsible for synthesis, folding, trafficking and maturation of proteins, as well as cholesterol synthesis. It has been established that stress in endoplasmic reticulum (ER) induces cell death (Takemoto et al. 2011). The quality control of newly synthesized proteins by the ER is essential for normal cell function and survival. However, integrity of the ER is often perturbed by accumulation of unfolded or misfolded proteins, leading to the unfolded protein response (UPR). The UPR is a signaling network consisting of three branches that are initiated by three different ER transmembrane receptors, i.e., pancreatic ER kinase (PKR)-like ER kinase (PERK), activating transcription factor 6 (ATF6) and inositol-requiring enzyme 1 (IRE1) (Ron and Walter 2007). Normally, these receptors remain in an inactive state because of their binding with glucose-regulated protein (GRP78). However, ERS lead to the dissociation of GRP78 from these receptors and then trigger the UPR, which initially aims at rebuilding cellular homeostasis by restoring the normal functions of the ER if ERS is moderate and transient, but eventually puts cells to death if ERS is inordinate or protracted (Rao et al. 2004; Xu et al. 2005). CCAAT/enhancer-binding protein–homologous protein (CHOP) is a proapoptotic transcription factor that suppresses the transcription of Bcl-2, which can be induced by a combination of the PERK/ATF4 and ATF6 pathways (Anding et al. 2007; Hetz et al. 2006; Moenner et al. 2007). CHOP overexpression promotes cell death, while deletion of the CHOP gene results in the attenuation of cell death induced by ER stress (Friedman 1996; McCullough et al. 2001).

In recent years, natural products have been increasingly recognized as new remedies for enhancing the efficacy and alleviating the adverse effects of tumor therapies (Surh 2003). Recent study has demonstrated that the natural flavonoid wogonin triggered apoptosis in human osteosarcoma U-2 OS cells through the ERS (Lin et al. 2011). Another natural flavonoid compound oroxylin A activates the UPR in human hepatocellular carcinoma HepG2 cells (Xu et al. 2012).

V8 (7-{4-[Bis-(2-hydroxy-ethyl)-amino]-butoxy}-5-hydroxy-8-methoxy-2-phenyl-chromen-4-one) is a newly synthesized flavonoid with the similar structure of wogonin. The V8 (**1**) was synthesized from natural product wogonin (**2**) through two steps as indicated in Fig. 1. Initially, the phenolic hydroxy group at the C7 of Wogonin was alkylated with 1, 4-dibromobutane in acetone in the presence of K_2CO_3. Then diethanolamine were coupled with the halogenated hydrocarbons (**3**) to afford V8. It was identified by IR, 1H-NMR, MS and elemental analysis. The purity was 99.51 % determined with HPLC. mp:241–243 °C.

Considering the aforementioned factors, in this study, we also addressed the effect of V8 on the apoptosis inducing of human hepatocellular carcinoma HepG2 cells and transplanted mice H22 liver carcinomas. Our findings also shed light on the molecular mechanism by which V8 induces apoptosis in hepatocellular carcinoma cells in vitro and in vivo.

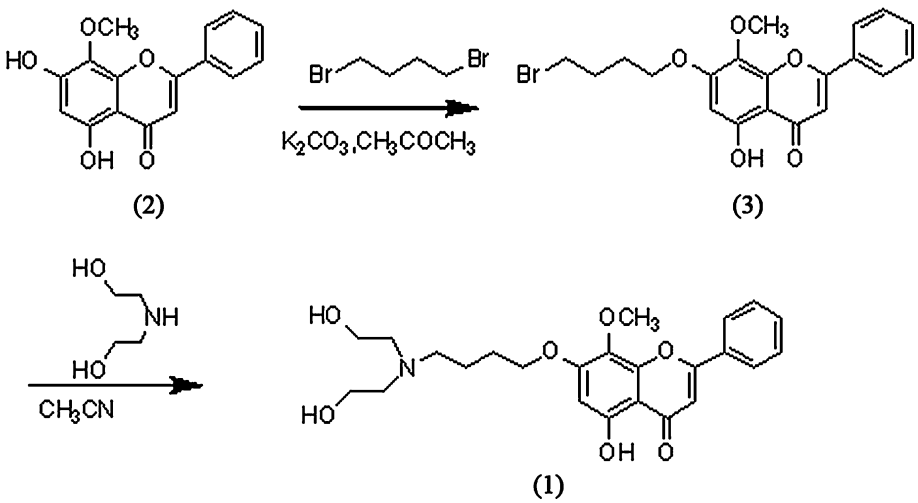

Fig. 1 The synthetic route of V8. *1* Molecular structure of V8 ($C_{24}H_{29}NO_7$, MW = 443.49), *2* Molecular structure of wogonin, *3* halogenated hydrocarbons

Materials and methods

Materials

V8 (purity >99.5 %) was applied in DMSO to 0.1 M and stored at −20 °C. The concentrations used here were 10, 20 and 30 μM in vitro and freshly diluted with DMEM to final concentration. Controls were treated with the same amount of DMSO (0.1 %) as used in the corresponding experiments. MTT [3-(4, 5-dimethylthiazol-2-yl)-2, 5-diphenytetrazoliumbromide] was obtained from Fluka chemical corp (Ronkonkoma, NY) and was dissolved in 0.01 M PBS. N-acetyl-L-cysteine (NAC) was purchased from Sigma-Aldrich (USA) and dissolved in sterile water. Primary antibodies of PERK, p-PERK, eIF2α, p-eIF2α, ATF4, Pro-caspase3, Pro-caspase9, Bcl-2, Noxa, COX-IV, Cyt-c, Bax and β-actin were obtained from Santa Cruz Biotechnology (California, USA). Antibodies of AIF, Bad and Bim were purchased from Cell Signaling Technology (Beverly, MA, USA). Antibodies of CHOP, GRP78 and Histones were the products of Bioworld (USA).

Cell culture and animals

The human hepatoma HepG2 cell line was purchased from Cell Bank of Shanghai Institute of Biochemistry and & Cell Biology, Chinese Academy of Sciences. Cells were grown in DMEM medium (Gibco, USA) supplemented with 10 % fetal bovine serum (Sijiqing, Hangzhou, China), 100 units/ml penicillin and 100 μg/ml streptomycin. Exponentially growing cultures were maintained in a humidified atmosphere of 5 % CO_2 at 37 °C.

Specific pathogen-free female Kunming mice with body weights of 18–22 g were used. All the mice were obtained from Shanghai Slac Laboratory Animal Co. Ltd. (Ureshino et al. 2011). The animals were maintained under controlled temperature (23 ± 2 °C, 55 ± 5 % humidity) and daily light intensity (12 h of light), and had free access to standard rodent diet and water throughout the experimental period.

MTT assay

The HepG2 cells were plated on 96-well plates with 1×10^4/well in 100 μL culture medium. The cells were incubated overnight and then exposed to drug at different concentrations for 24 h. Subsequently, 20 μl/well of MTT solution (5 mg/ml) was added. Plates were incubated at 37 °C in a 5 % CO_2 atmosphere; after 4 h, the supernatants were removed and 100 μL/well DMSO was added to dissolve formazan crystals. Plates were placed on an orbital shaker for 2 min, and the absorbance was recorded at 570 nm (EL800, BIO-TEK Instruments Inc.). Cell viability was determined based on mitochondrial conversion of MTT to formazan. Inhibition ratio (%) was calculated using the following equation:

$$I(\%) = \left(\frac{A_{\text{control}} - A_{\text{treated}}}{A_{\text{control}}}\right) \times 100$$

IC_{50} value was taken as the concentration that caused 50 % inhibition of cell viabilities and calculated by the logit method.

Cell morphology

To detect morphological evidence of apoptosis, cell nuclei were visualized following DNA staining with the fluorescent dye DAPI (Santa Cruz, USA). Briefly, cells were cultured in 6-well tissue culture plates and treated with the indicated concentration of drug. At the end of incubation, the cells were fixed with 4 % paraformaldehyde for 20 min and incubated with DAPI (1 μg/mL) for 10 min. After washing with PBS, fluorescent intensity of cells with dye was observed and compared under fluorescence microscope (Olympus, Japan) with a peak excitation wavelength of 340 nm.

Annexin V/PI staining

HepG2 cells were harvested after treatment and stained with the Annexin V/PI Cell Apoptosis Detection Kit (KeyGen Biotech, Nanjing, China) according to the manufacturer's instructions. Data acquisition and analysis were performed with a Becton–Dickinson FACSCalibur flow cytometer using CellQuest software at Ex./Em.−488/530 nm. The cells in early stages of apoptosis were annexin V-positive and PI-negative, whereas the cells in the late stages of apoptosis were both annexin V and PI positive.

Measurement of ROS formation

According to the method described previously (Lluis et al. 2007), the level of intracellular ROS was detected using fluorescent dye 2, 7-dichlorofluorescein-diacetate (DCFH-DA, Beyotime Institute of Biotechnology, China) sensitively. The HepG2 cells were pretreated with 10, 20 and 30 μM of V8 for 12 h. The cells were collected and incubated with 100 mM DCFH-DA attenuated with serum-free medium for 30 min at 37 °C in the dark. After washed by serum-free, the fluorescence intensity was measured by FACSCalibur flow cytometry (Becton–Dickinson) at Ex./Em. −488/525 nm.

Detection of intracellular calcium level

V8-treated (10, 20 and 30 μM for 12 h) cells were loaded with 1 μM Fluo-3 AM (Beyotime, China) which combined

with Ca^{2+} and produced strong fluorescence. After incubating for 60 min at 37 °C in the dark, the cells were resuspended with PBS and the fluorescence intensity were measured by FACSCalibur flow cytometry (Becton–Dickinson) at Ex./Em. −488/525 nm.

Mitochondrial transmembrane potential (ΔΨm) assessment

The electrical potential difference across inner ΔΨm was monitored using the ΔΨm-specific fluorescent probe JC-1 (KeyGen Biotechnology Co. Ltd., China) which exists as a monomer with an emission at 530 nm (green fluorescence) at low membrane potential but forms J-aggregates with an emission at 590 nm (red fluorescence) at higher potential.

Briefly, the HepG2 cells were treated with V8 for 24 h. Then the cells were harvested and re-suspended in DMEM medium at a density of 0.5×10^6 cells/ml. After incubating with JC-1 for 30 min at 37 °C, the cells were resuspended in washing buffer and analyzed by flow cytometry. Relative fluorescence intensity was monitored with the flow cytometry (FACS Calibur, Becton–Dickinson), and analyzed by the software Modfit and CellQuest (BD Biosciences, Franklin Lakes, NJ) with settings of FL1 (FITC, green) at 530 nm and FL2 (PE, red) at 590 nm.

Subcellular fractionation

The mitochondrial and cytosolic fractions of cells were performed using cytosol/mitochondria fractionation kit (KeyGen Biotech, China) according to the following protocol. The cells were treated with different concentrations of V8 for 24 h and were harvested and incubated in 100 μL ice-cold mitochondrial lyses buffer for 10 min. Cell suspension was homogenized for strike with a tight pestle. The homogenate was subjected to centrifuging at 600 g for 10 min at 4 °C to remove nuclei and unbroken cells. Then the supernatant was collected and centrifuged again at 12,000 g for 30 min at 4 °C to obtain the cytosol (supernatant) and mitochondria (deposition) fraction. Samples of cytosol and mitochondria were dissolved in lyses buffer at −20 °C.

Transient transfection with CHOP small interfering RNA (siRNA)

For knockdown experiments, HepG2 cells grown to 60 % confluence were cultured in serum-free medium for 4 h. Then either CHOP siRNA (20 pmol/μL) or control siRNA was added into the cells using Lipofectamine 2000 (Invitrogen, Carlsbad, CA). Four hours later, the cells were cultured in the blood serum medium for 24 h and harvested for further experiment.

Western blot analysis

Twenty-four hours after treatment with V8, the HepG2 cells were lysed with a mixture of lysis buffer (50 mM Tris–HCl; 150 mM NaCl; 1 mM EDTA; 1 % NP-40; and 0.1 mM NaF, pH7.6) and a proteinase inhibitor cocktail (0.2 mM phenylmethanesulfonyl fluoride, 1 mM dithiothreitol and 0.1 mM leupeptin). The concentration of total proteins was measured using the BCA assay method with a Varioskan spectrofluorometer and spectrophotometer (Thermo, Waltham, Massachusetts) at 562 nm.

Protein (with 100 μg) from each sample was loaded into each lane of the SDS-PAGE (10 % gel), stacked at 70 V for 30 min and separated at 110 V and transferred to nitrocellulose membranes at 20 V. After blocking with 1.0 % BSA (Roche, Mannheim, Germany) for 60 min at 37 °C, the membranes were incubated with primary antibodies for 60 min at 37 °C and overnight at 4 °C, which was followed by incubation with IRDye 800-labeled secondary antibodies (KPL, Gaithersburg, MD, USA) for 60 min at 37 °C in the dark. Subsequently, the intensities of protein bands were detected at 562 nm using an Odyssey Infrared Imaging System (LI-COR, Lincoln, NE, USA).

Effect of V8 on the growth of transplanted tumor H22 in mice

Female Kunming mice with body weight of 18–22 g were transplanted with H22 cells in oxter. Twenty-four hours after inoculation, the mice were divided randomly into five groups (with 10 mice/group): saline control group, V8 10 mg/kg group, V8 20 mg/kg group, V8 40 mg/kg group and wogonin 40 mg/kg group. All groups were administered intravenously every 2 days.

Eight days later, all mice were killed and weighed simultaneously, and the tumor was segregated, weighed and stored in −80 °C. Tumor inhibitory ratio I (%) was calculated by the following formula:

$$I(\%) = \left(\frac{W_{\text{control}} - W_{\text{treated}}}{W_{\text{control}}}\right) \times 100$$

W_{treated} and W_{control} were the average tumor weight of the treated and control group, respectively.

Statistical analysis

Data are expressed as the mean of three experiments, each in triplicate samples for individual treatments or dosage. We use the software of SigmaPlot, Graphpad and Excel to analyze these data. All comparisons of data were made using Student's t test and were considered to be statistically significant at $p < 0.05$. Values are represented as the Mean ± SD.

Results

V8 inhibits hepatocarcinoma proliferation in vivo and in vitro

For assessing in vitro cell viability, MTT assays were performed to ascertain the anti-proliferative effect of V8 on the HepG2 cells. As shown in Fig. 2a, after 24-h treatment, V8 obviously reduced the number of viable cells at an IC_{50} value of 23 μM. In addition, a clear concentration–effect relationship was established. As shown in Fig. 2b, all treated groups showed inhibitory effects. Compared with the control group, tumor's weight in the V8 40 mg/kg treatment group was decreased by 63 %. This effect was far stronger than 40 mg/kg wogonin regimens, in which the inhibitory rate was 38 %. V8 10 mg/kg and 20 mg/kg treatments resulted in 26 and 41 % of tumor weight loss, respectively. At the meantime, no significant changes in body weight, liver, spleen and thymus was found in either the treatment or control group (data were not shown). The results showed that V8 inhibited the transplanted mice H22 liver carcinomas in a dose-dependent manner without significant side effect.

V8 induces apoptosis in HepG2 cells

Whether the antiproliferative activities of V8 could be due to the induction of apoptosis was addressed. In order to confirm the occurrence of apoptosis in HepG2 cells after the treatment of V8, the treated cells were stained by DAPI. Apoptotic cells were recognized by the condensed, fragmented, degraded nuclei and apoptotic body. Under the fluorescent microscope, untreated HepG2 cells were stained equably with blue fluorescence, demonstrating the steady chromatinic distribution in nucleolus. HepG2 cells treated with V8-emitted bright fluorescence, which meant that chromatin agglutination, nucleolus pyknosis and apoptosis were investigated. There was a significant difference between the V8-treated groups and the same connection of wogonin group. With the increasing doses of V8, more and more nuclear fragments were disintegrated and formed (Fig. 3a). Another flow cytometric analysis also gave the similar results (Fig. 3b). Exposing HepG2 cells to 10, 20 and 30 μM of V8 and 30 μM of wogonin for 24 h enhanced the percentage of apoptosis cells. Compared with control group (5.9 ± 2.9 %), apoptotic rate of V8 10-, 20- and 30-μM-treated cells were increased to 21.4 ± 3.3, 46.5 ± 2.4 and 53.5 ± 2.7 %, respectively. While apoptotic rate of wogonin 30-μM-treated cells was less than 10 % (7.62 ± 2.44 %). The results of our experiments illustrated that V8 possesses more potent anti-cancer activities. Not only because V8 induced hepG2 apoptotic death in a concentration-dependent manner, but also it induced human hepatocellular carcinoma HepG2 cells apoptosis with an even stronger effect than that of wogonin.

V8 triggers ROS generation

Accumulation of ROS can lead to ER stress, mitochondrial dysfunction and initiate apoptosis (Sanges and Marigo 2006). To demonstrate the effects of V8 on ROS induction, we determined the production of ROS with a probe carboxy-H_2DCFDA, which is converted to a green fluorescent product, carboxy-DCF, via oxidation. A rapid production of ROS occurred after the exposure of HepG2 cells to V8 (Fig. 4a). In addition, NAC, a ROS scavenger, partly reduced the accumulation of ROS induced by V8. To further determine whether ROS was involved in the apoptosis

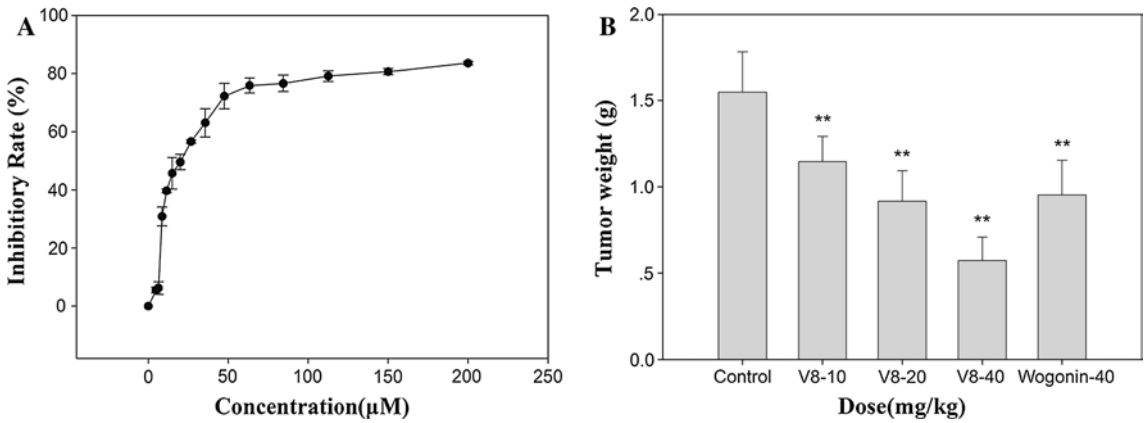

Fig. 2 Inhibitory effect of V8 in vivo and in vitro. **a** HepG2 cells were treated with various concentration of V8 for 24 h. Cell viability was determined using MTT assay. Data were shown as Mean ± SD ($n = 3$). **b** The transplanted mice H22 liver carcinomas were treated with 10, 20 and 40 mg/kg of V8 by i.v. once every 2 days. Control was treated with normal saline, and positive control was treated with 40 mg/kg of wogonin by i.v. once every 2 days. Results were given as Mean ± SD ($n = 10$)

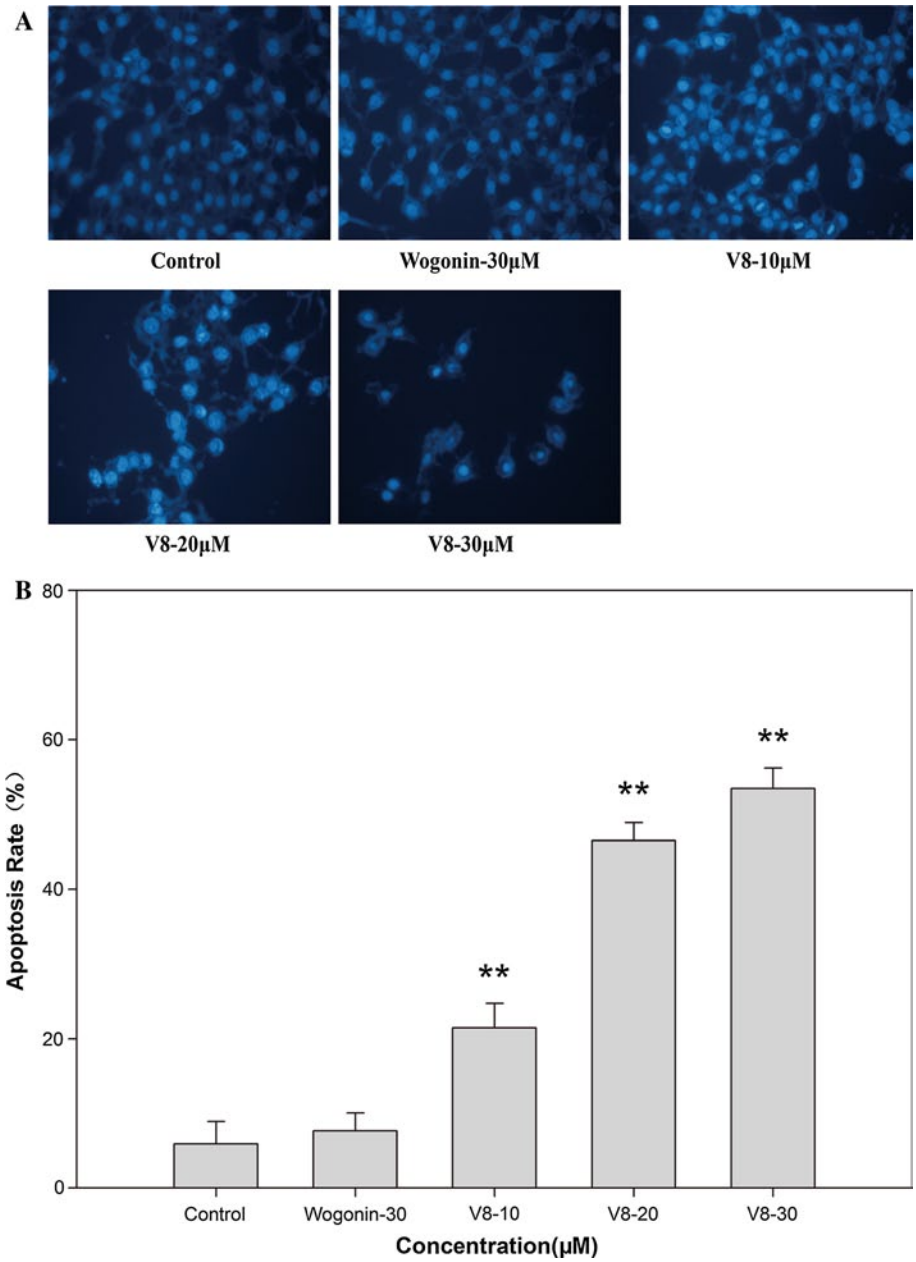

Fig. 3 Apoptosis induced by V8 in HepG2 cells. **a** Cells were treated with 10, 20 and 30 μM V8 for 24 h and then were stained with DAPI. **b** The apoptotic rates of HepG2 cells induced by V8 were analyzed by flow cytometry. Data were shown as Mean ± SD for three independent experiments ($^{*}p < 0.05$ and $^{**}p < 0.01$ compared with control)

induction by V8, HepG2 cells were pretreated with/without NAC and then exposed to the compound. Annexin V/PI staining showed that V8-induced ROS-mediated apoptosis was partly inhibited by NAC (38.0 ± 3.0 % in V8 30 μM group vs. 22.0 ± 2.9 % in NAC+V8 30 μM group, Fig. 4b). These data suggested that the accumulation of ROS plays an important role in V8-induced apoptosis.

V8 induces apoptosis via initiating ER stress

Ca^{2+} overloading was an obvious signal to prove the activity of endoplasmic reticulum stress (Kim et al. 2008). The production of Ca^{2+} was showed in Fig. 5a. An increased fluorescence correlated with an up-regulating Ca^{2+} level was observed in HepG2 cells with a dose-dependent manner. To study the effect of ER stress in V8 inducing apoptosis, the cells were exposed to V8 for 24 h and harvested for western blot analysis regarding ER stress pathway-related proteins expression. Results were shown in Fig. 5c, which indicated that V8 promoted the protein levels of CHOP, GRP78, ATF4, p-PERK and p-eIF2α and decreased PERK, while had no effect on eIF2α. To confirm the mechanism of apoptosis in vivo, we detected the proteins in transplanted mice H22 liver carcinomas tumor tissues and the similar results were found (Fig. 5d). These data showed that V8 initiated ER stress both in vitro and in vivo.

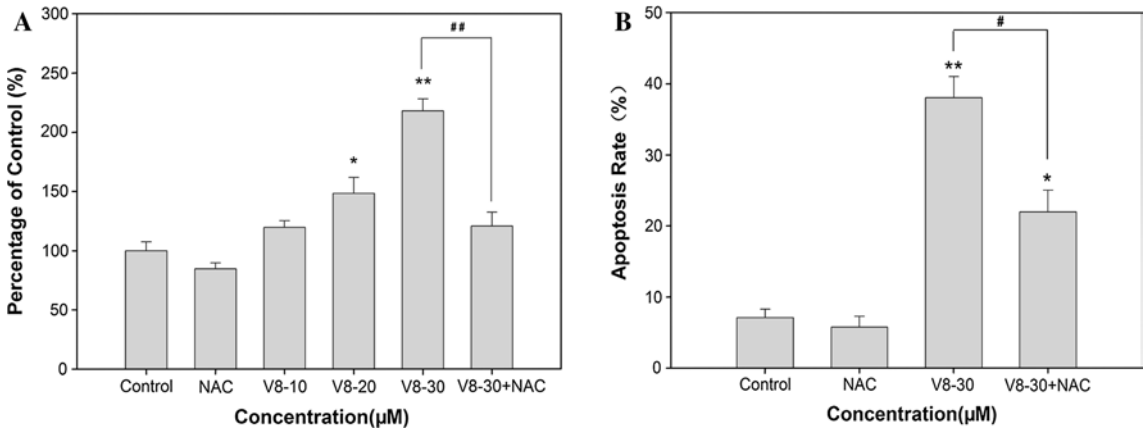

Fig. 4 V8 affected the productions of ROS. **a** Cells were pretreated with/without 5 mM NAC for 1 h, and then exposed with/without V8 for 12 h. Finally, the ROS level was detected by flow cytometry. **b** Cells were pretreated with/without 5 mM NAC for 1 h and treated with/without 30 μM V8 for 12 h. The apoptosis were analyzed with flow cytometry. Values were Mean ± SD for at least three independent experiments ($^{*}p < 0.05$ and $^{**}p < 0.01$ compared with control; $^{\#}p < 0.05$ and $^{\#\#}p < 0.01$ compared with V8-treated group)

CHOP is known as a crucial factor that mediates ER stress-induced apoptosis (Zinszner et al. 1998). To examine the importance of CHOP in V8-induced apoptosis, HepG2 cells were transiently transfected with control or CHOP siRNA. As shown in Fig. 5b, percentages of apoptosis cells were significantly reduced in V8+CHOP-siRNA-treated group (39.2 ± 1.1 % in V8+control-siRNA-treated group vs. 21.6 ± 4.9 % in V8+CHOP-siRNA-treated group). The results suggested that CHOP have an important effect on V8-induced apoptosis.

V8 activates the mitochondrial apoptosis pathway

JC-1 is a mitochondrial ΔΨ-sensitive dye. When mitochondrial ΔΨ is high, JC-1 accumulates in the matrix of mitochondria by forming J-aggregates with red fluorescence. However, when mitochondrial ΔΨ is low, JC-1 becomes monomer with green fluorescence. The ratio of green and red fluorescence indicates depolarization percentage of mitochondria. Results showed a remarkable increase in green fluorescence of JC-1 monomers in V8-treated cells (Fig. 6a). The percentage of cells with green fluorescence increased to 27.0 ± 1.7, 52.2 ± 2.8 and 70.6 ± 3.5 % with V8 at the concentration of 10, 20 and 30 μM, respectively. In addition, mitochondrial dysfunction associated with ER stress-mediated cell death induces the pro-apoptotic proteins such as Cyt-c releasing from the mitochondria to the cytosol and subsequently causing a caspase-dependent apoptosis (Li et al. 2006). In the present study, after the HepG2 cells were treated with different concentrations of V8 for 24 h, the amount of Cyt-c significantly decreased in mitochondria while increased in cytosol, which aimed to caspase-dependent apoptosis (Fig. 6b). Upon induction of apoptosis, AIF translocates from the mitochondria to the nucleus, causes DNA fragmentation and leads to chromatin condensation in a caspase-independent manner(Ola et al. 2011). In Fig. 6b, AIF in V8-treated group was found transferred from mitochondria to nucleus, which indicated V8 induced the dysfunction of mitochondria, finally resulted in caspase-independent apoptosis.

Subsequently, western blot analysis evaluated the molecular effects of V8-induced apoptosis in vitro and in vivo. There was significant elevation in the percentages of Bad, Bim, Noxa and Bax, while a decreased level of Bcl-2. Procaspase3 and Pro-caspase9 was also observed in the treated HepG2 cells (Fig. 6c). The same effects of V8 treatment on the apoptosis-related proteins in the transplanted mice H22 liver carcinomas were found (Fig. 6d). In addition, the level of caspase8 which was representative for extrinsic pathway-induced apoptosis was not changed (data were not shown)(Kruidering and Evan 2000).

Discussion

Hepatocellular carcinoma (HCC) is a malignant tumor with affecting about one million people around the world every year (Motola-Kuba et al. 2006). Traditional Chinese medicines have been recently recognized as a new source of anticancer drugs and new chemotherapy adjuvant to enhance the efficacy of chemotherapy and to ameliorate the side effects of cancer chemotherapies. Scutellaria baicalensis is one of the most popular and multi-purpose herbs used in China traditionally for treatment of cancer, inflammation, hypertension, cardiovascular diseases, bacterial and viral infections. Wogonin is one of the major constituents of Scutellaria baicalensis and exerts anti-oxidant activity, which may, in part, underlie its anti-inflammatory, anti-cancer, antiviral

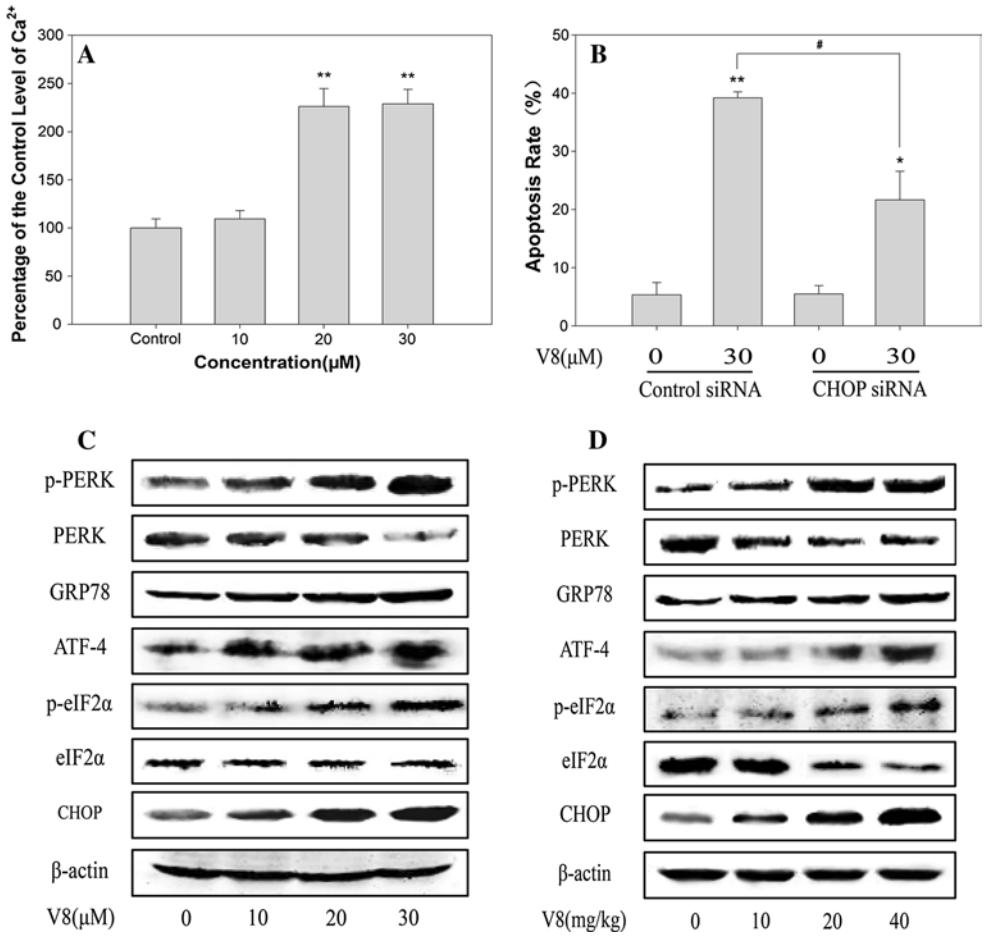

Fig. 5 V8 induced apoptosis by initiating ER Stress. **a** Cells were treated with 10, 20 and 30 μM V8 for 12 h, and the Ga^{2+} level was detected. Data are Mean ± SD for three independent experiments ($^{*}p < 0.05$ and $^{**}p < 0.01$ compared with control). **b** HepG2 cells were treated in serum-free medium for 4 h, then transfected with control siRNA or CHOP siRNA and incubated for 4 h. After cultured in blood serum culture medium for 12 h, the cells were treated with/without 30 μM V8 for 24 h. Then the apoptosis was detected with annexin V/PI double staining. Data were Mean ± SD for three independent experiments ($^{*}p < 0.05$ and $^{**}p < 0.01$ compared with control-siRNA-transfected group; $^{\#}p < 0.05$ and $^{\#\#}p < 0.01$ compared with V8 + control-siRNA-treated group). **c** HepG2 cells were incubated with 10, 20 and 30 μM V8 for 24 h and the protein of PERK, p-PERK, GRP78, ATF4, eIF2α, p-eIF2α and CHOP were analyzed by western blotting. **d** Proteins including PERK, p-PERK, GRP78, ATF4, eIF2α, p-eIF2α and CHOP come from transplanted mice H22 liver carcinomas tissues were detected by western blotting

and neuroprotective actions (Li-Weber 2009). We modified the structure of wogonin and finally got a new compound, which named V8. In our studies, V8 showed inhibitory effect on the transplanted mice H22 liver carcinomas. Results demonstrated that the tumor inhibitory effect of 40 mg/kg/2 days of V8 treatment was stronger than that of 40 mg/kg/2 days of wogonin treatment (63 vs. 38 %). Recent research found that wogonin induces apoptosis via ROS-mediated ER stress pathway (Lin et al. 2011). V8, bears a structural similarity to wogonin, has been shown to inhibit tumor cell growth. In this research, we discovered the fundamental mechanisms of V8 fighting against hepatocellular carcinoma.

Apoptosis is accompanied by various morphological changes, including nuclear condensation, apoptotic bodies, DNA fragmentation and cell surface changes (Noori and Hassan 2012). Nuclear morphology in the HepG2 cells was analyzed using DAPI staining; the externalization of apoptosis was detected using Annexin V/PI staining and sorted with a flow cytometer. These experiments indicated that V8 caused chromatin condensation and externalization of apoptosis in the HepG2 cells.

The mitochondrial pathway is one of apoptotic types, especially in ROS-induced apoptosis. ROS is mainly generated in the mitochondria (King et al. 2004), but mitochondria is not the only cellular organelles that response to oxidative stress. Recent studies suggest that the endoplasmic reticulum (ER) is quite sensitive to oxidative damage (Wang et al. 2007) and may also play an important role in the response to oxidative stress-induced damage (Sanges and Marigo 2006). Various physiopathological conditions like hypoxia, ER-Ca^{2+}

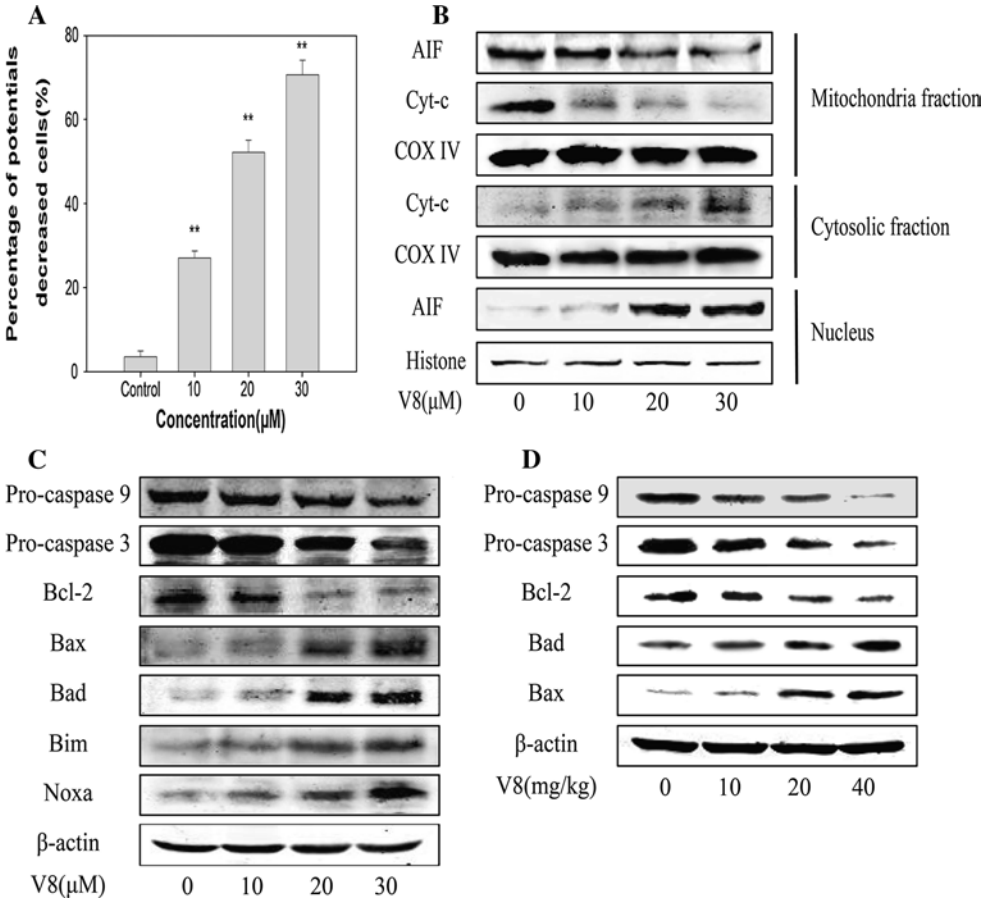

Fig. 6 V8 activates the mitochondrial apoptotic pathway. **a** Cells were exposed to V8 (10, 20 and 30 μM) for 24 h and then stained with JC-1. The percentage of ΔΨ collapsed cells was analyzed by flow cytometry. Data were mean ± SD for at least three independent experiments ($^{*}p < 0.05$ and $^{**}p < 0.01$ compared with control). **b** Effect of V8 on Cyt-c and AIF in HepG2 cells. The cells were treated with V8 (10, 20 and 30 μM) for 24 h. Mitochondrial, cytosolic and nuclei fractions were subjected to western blot analysis. **c** HepG2 cells were incubated with 10, 20 and 30 μM V8 for 24 h. The protein of Pro-caspase9, Pro-caspase3, Bcl-2, Bax, Bad, Bim and Noxa was analyzed with western blotting. **d** The proteins of Pro-caspase9, Pro-caspase3, Bcl-2, Bax and Bad come from transplanted mice H22 liver carcinomas tissues were detected by western blotting

depletion, oxidative damage including ROS-mediated, hypoglycemia and viral infections may affect ER homeostasis and interfere with proper protein folding, ultimately causing an imbalance between protein folding load and capacity. This cellular condition is known as'ER stress.' The ER responds to these perturbations by activating an integrated signal transduction pathway, called the unfolded protein response (UPR). The UPR is primarily tailored to reestablish ER homeostasis by coordinating the temporal shutdown in protein translation along with a complex program of gene transcription that leads to the up-regulation of components of the ER folding machinery and ER quality control, like the ER-associated degradation (ERAD) pathway. However, when ER stress is too severe or cannot be solved, the UPR turns from a pro-survival to a pro-death response, usually, but not uniquely, culminating in the activation of intrinsic apoptosis (Verfaillie et al. 2010). In this study, we found the level of ROS in the V8-treated HepG2 cells increased. Further experiment showed that V8-induced apoptosis was partly inhibited by NAC, a ROS production inhibitor. The results indicated that V8 induce apoptosis partly though ROS pathway.

Change of ER Ca^{2+} stores is involved in ER stress-mediated apoptosis (Kim et al. 2008). We have known that ER stress often stimulated a release of Ca^{2+} into the cytosol, followed by uptake of Ca^{2+} into mitochondria, mitochondrial fission and release of cytochrome c, precipitating apoptosis(Verfaillie et al. 2010). The apoptotic cross-talk between the ER and the mitochondria requires calcium signaling from the ER to the mitochondria, which is inhibited by Bcl-2 and promoted by Bax (Hotokezaka et al. 2009). In this study, we observed that V8 induced intracellular Ca^{2+} overloading, indicating that alterations in Ca^{2+} homeostasis were involved in V8-induced apoptosis. We further investigated specific markers of ER stress such as GRP78, p-PERK, p-eIF2α, ATF4 and CHOP. In mammalian cells, ER stress is initiated by three ER transmembrane proteins: PERK, IRE1 and ATF6. These three ER stress sensors trigger divergent and convergent signaling cascades that lead to adaptation or cell death. Generally, these branches function as a whole upon the ERS. For the ERS sensor GRP78, the regulators PERK, p-PERK (thr981), eIF2α, p-eIF2α (Ser51) and ATF4 together with the mediator CHOP constitute an essential and dominant branch (Lin et al. 2007; Oyadomari and Mori 2004; Szegezdi et al. 2006; Tabas and Ron 2011; Yoshida et al. 2003). After treatment of V8, the PERK-eIF2α-ATF4 signaling pathway in vivo and in vitro was activated obviously. CCAAT/enhancer-binding protein-homologous protein

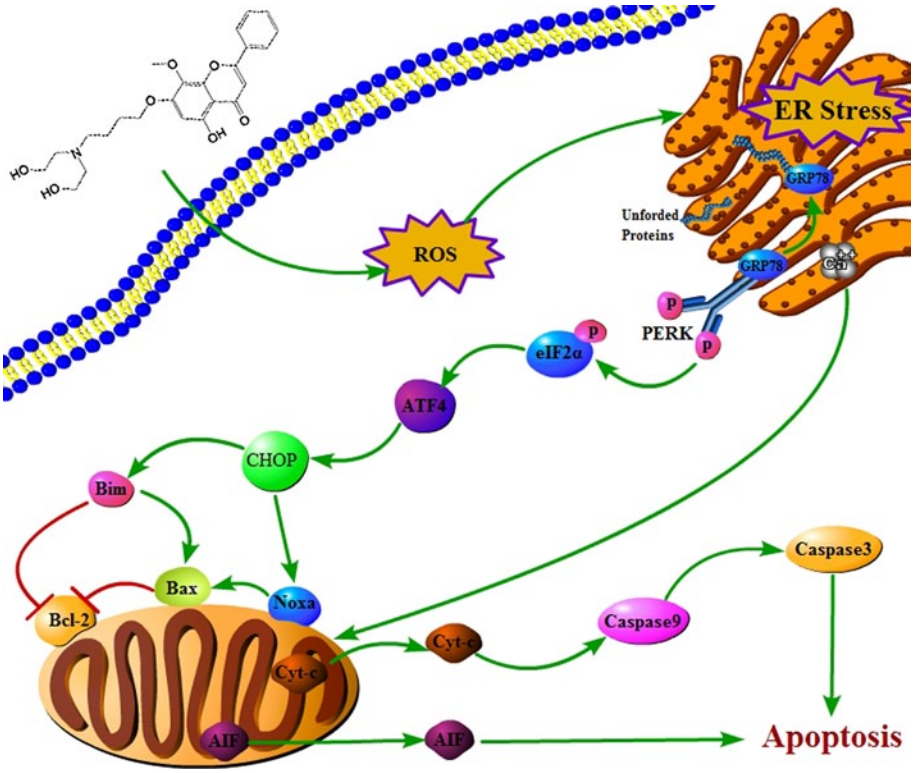

Fig. 7 V8 induced apoptosis via ROS-dependent ER stress pathway. V8 induced ROS trigger UPR in ER. Canonical signaling via the PERK-eIF2a-ATF4 branch of the UPR induced the pro-apoptotic transcription factor CHOP, which in turn mediated mitochondrial apoptosis through the up-regulation of BH-3 only proteins. As a result, Cyt-c and AIF were released from the pool of mitochondria. This process finally triggered a complex downstream pathway activating apoptosis

(CHOP/GADD153) is a pro-apoptotic transcription factor that suppresses the transcription of Bcl-2, which can be induced by a combination of the PERK/ATF4 and ATF6 pathways (Anding et al. 2007; Hetz et al. 2006; Moenner et al. 2007). CHOP overexpression promotes cell death, while deletion of the CHOP gene results in the attenuation of cell death induced by ER stress (Friedman 1996; McCullough et al. 2001). Overexpression of CHOP inhibits Bcl-2 protein expression and translocation of Bax protein from the cytosol to mitochondria (Oyadomari and Mori 2004). CHOP can transcriptionally induce the expression of Bad, Bim and Noxa. Bim connects with Bcl-2 and Bax to enhance the activation of mitochondrial voltage-dependent anion channel and then leads to release of apoptogenic factors from the mitochondria (Sugiyama et al. 2002). Another BH-3 only protein Noxa induces Cyt-c release from mitochondria through activation of Bax(Li et al. 2006). The BH-3 domain of Bad binds and inactivates Bcl-2 at the outer mitochondrial membrane, thereby promoting cell death(Ola et al. 2011). Results showed that V8 caused Ca^{2+} overloading and mitochondrial dysfunction. It triggered caspase-dependent and independent apoptosis subsequently. More importantly, the molecular mechanisms of V8-induced apoptosis in vitro were verified in vivo. CHOP-specific siRNA is designed to knock down CHOP/GADD 153 gene expression. Our further study suggested that CHOP-siRNA-rescued apoptosis was induced by V8, but not completely. It is indicated that there have been another ER-independent way inducing apoptosis. All those results demonstrated that V8 induced apoptosis in HepG2 cells through activating ER Stress.

In summary, V8 exerts strong hepatocellular carcinoma growth inhibition in vivo and in vitro by inducing apoptosis. The mechanisms were ROS triggered ER stress (Fig. 7) which was similar with wogonin while V8 exhibited even more active effects. V8 might become a promising therapeutic agent against hepatocellular carcinoma cancer.

Acknowledgments This work was supported by Program for Changjiang Scholars and Innovative Research Team in University (IRT1193), the Project Program of State Key Laboratory of Natural Medicines, China Pharmaceutical University(No. JKGZ201101), the National Science & Technology Major Project (No.2012ZX09304-001) and Natural Science Foundation of Jiangsu province (No.BK2009297 and No.BK2010432).

References

Anding AL, Chapman JS, Barnett DW, Curley RW Jr, Clagett-Dame M (2007) The unhydrolyzable fenretinide analogue 4-hydroxybenzylretinone induces the proapoptotic genes GADD153 (CHOP) and Bcl-2-binding component 3 (PUMA) and apoptosis that is caspase- dependent and independent of the retinoic acid receptor. Cancer Res 67(13):6270–6277. doi:10.1158/0008-5472.CAN-07-0727

Bruix J, Llovet JM (2009) Major achievements in hepatocellular carcinoma. Lancet 373(9664):614–616. doi:10.1016/S0140-6736(09)60381-0

El-Serag HB (2011) Hepatocellular carcinoma. N Engl J Med 365(12):1118–1127. doi:10.1056/NEJMra1001683

Friedman AD (1996) GADD153/CHOP, a DNA damage-inducible protein, reduced CAAT/enhancer binding protein activities and increased apoptosis in 32D c13 myeloid cells. Cancer Res 56(14):3250–3256

Gish RG, Baron A (2008) Hepatocellular carcinoma (HCC): current and evolving therapies. IDrugs 11(3):198–203

Hetz C, Bernasconi P, Fisher J et al (2006) Proapoptotic BAX and BAK modulate the unfolded protein response by a direct interaction with IRE1alpha. Science 312(5773):572–576. doi:10.1126/science.1123480

Hotokezaka Y, van Leyen K, Lo EH et al (2009) alphaNAC depletion as an initiator of ER stress-induced apoptosis in hypoxia. Cell Death Differ 16(11):1505–1514. doi:10.1038/cdd.2009.90

Jemal A, Bray F, Center MM, Ferlay J, Ward E, Forman D (2011) Global cancer statistics. CA Cancer J Clin 61(2):69–90. doi:10.3322/caac.20107

Kim I, Xu W, Reed JC (2008) Cell death and endoplasmic reticulum stress: disease relevance and therapeutic opportunities. Nat Rev Drug Discov 7(12):1013–1030. doi:10.1038/nrd2755

King A, Gottlieb E, Brooks DG, Murphy MP, Dunaief JL (2004) Mitochondria-derived reactive oxygen species mediate blue light-induced death of retinal pigment epithelial cells. Photochem Photobiol 79(5):470–475

Kruidering M, Evan GI (2000) Caspase-8 in apoptosis: the beginning of "the end"? IUBMB Life 50(2):85–90. doi:10.1080/713803693

Li J, Lee B, Lee AS (2006) Endoplasmic reticulum stress-induced apoptosis: multiple pathways and activation of p53-up-regulated modulator of apoptosis (PUMA) and NOXA by p53. J Biol Chem 281(11):7260–7270. doi:10.1074/jbc.M509868200

Lin JH, Li H, Yasumura D et al (2007) IRE1 signaling affects cell fate during the unfolded protein response. Science 318(5852):944–949. doi:10.1126/science.1146361

Lin CC, Kuo CL, Lee MH et al (2011) Wogonin triggers apoptosis in human osteosarcoma U-2 OS cells through the endoplasmic reticulum stress, mitochondrial dysfunction and caspase-3-dependent signaling pathways. Int J Oncol 39(1):217–224. doi:10.3892/ijo.2011.1027

Li-Weber M (2009) New therapeutic aspects of flavones: the anticancer properties of scutellaria and its main active constituents wogonin baicalein and baicalin. Cancer Treat Rev 35(1):57–68. doi:10.1016/j.ctrv.2008.09.005

Llovet JM, Ricci S, Mazzaferro V et al (2008) Sorafenib in advanced hepatocellular carcinoma. N Engl J Med 359(4):378–390. doi:10.1056/NEJMoa0708857

Lluis JM, Buricchi F, Chiarugi P, Morales A, Fernandez-Checa JC (2007) Dual role of mitochondrial reactive oxygen species in hypoxia signaling: activation of nuclear factor-{kappa} B via c-SRC and oxidant-dependent cell death. Cancer Res 67(15):7368–7377. doi:10.1158/0008-5472.CAN-07-0515

McCullough KD, Martindale JL, Klotz LO, Aw TY, Holbrook NJ (2001) Gadd153 sensitizes cells to endoplasmic reticulum stress by down-regulating Bcl2 and perturbing the cellular redox state. Mol Cell Biol 21(4):1249–1259. doi:10.1128/MCB.21.4.1249-1259.2001

Moenner M, Pluquet O, Bouchecareilh M, Chevet E (2007) Integrated endoplasmic reticulum stress responses in cancer. Cancer Res 67(22):10631–10634. doi:10.1158/0008-5472.CAN-07-1705

Motola-Kuba D, Zamora-Valdes D, Uribe M, Mendez-Sanchez N (2006) Hepatocellular carcinoma. An overview. Ann Hepatol 5(1):16–24

Noori S, Hassan ZM (2012) Tehranolide inhibits proliferation of MCF-7 human breast cancer cells by inducing G0/G1 arrest and apoptosis. Free Radic Biol Med 52(9):1987–1999. doi:10.1016/j.freeradbiomed.2012.01.026

Ola MS, Nawaz M, Ahsan H (2011) Role of Bcl-2 family proteins and caspases in the regulation of apoptosis. Mol Cell Biochem 351(1–2):41–58. doi:10.1007/s11010-010-0709-x

Oyadomari S, Mori M (2004) Roles of CHOP/GADD153 in endoplasmic reticulum stress. Cell Death Differ 11(4):381–389. doi:10.1038/sj.cdd.4401373

Rao RV, Ellerby HM, Bredesen DE (2004) Coupling endoplasmic reticulum stress to the cell death program. Cell Death Differ 11(4):372–380. doi:10.1038/sj.cdd.4401378

Ron D, Walter P (2007) Signal integration in the endoplasmic reticulum unfolded protein response. Nat Rev Mol Cell Biol 8(7):519–529. doi:10.1038/nrm2199

Sanges D, Marigo V (2006) Cross-talk between two apoptotic pathways activated by endoplasmic reticulum stress: differential contribution of caspase-12 and AIF. Apoptosis 11(9):1629–1641. doi:10.1007/s10495-006-9006-2

Sugiyama T, Shimizu S, Matsuoka Y, Yoneda Y, Tsujimoto Y (2002) Activation of mitochondrial voltage-dependent anion channel by apro-apoptotic BH3-only protein Bim. Oncogene 21(32):4944–4956. doi:10.1038/sj.onc.1205621

Surh YJ (2003) Cancer chemoprevention with dietary phytochemicals. Nat Rev Cancer 3(10):768–780. doi:10.1038/nrc1189

Szegezdi E, Logue SE, Gorman AM, Samali A (2006) Mediators of endoplasmic reticulum stress-induced apoptosis. EMBO Rep 7(9):880–885. doi:10.1038/sj.embor.7400779

Tabas I, Ron D (2011) Integrating the mechanisms of apoptosis induced by endoplasmic reticulum stress. Nat Cell Biol 13(3):184–190. doi:10.1038/ncb0311-184

Takemoto K, Miyata S, Takamura H, Katayama T, Tohyama M (2011) Mitochondrial TRAP1 regulates the unfolded protein response in the endoplasmic reticulum. Neurochem Int 58(8):880–887. doi:10.1016/j.neuint.2011.02.015

Ureshino N, Aragane N, Nakamura T et al (2011) A fully integrated and automated detection system for single nucleotide polymorphisms of UGT1A1 and CYP2C19. Oncol Res 19(3–4):111–114

Verfaillie T, Garg AD, Agostinis P (2010) Targeting ER stress induced apoptosis and inflammation in cancer. Cancer Lett. doi:10.1016/j.canlet.2010.07.016

Wang X, Wang B, Fan Z, Shi X, Ke ZJ, Luo J (2007) Thiamine deficiency induces endoplasmic reticulum stress in neurons. Neuroscience 144(3):1045–1056. doi:10.1016/j.neuroscience.2006.10.008

Whittaker S, Marais R, Zhu AX (2010) The role of signaling pathways in the development and treatment of hepatocellular carcinoma. Oncogene 29(36):4989–5005. doi:10.1038/onc.2010.236

Xu C, Bailly-Maitre B, Reed JC (2005) Endoplasmic reticulum stress: cell life and death decisions. J Clin Invest 115(10):2656–2664. doi:10.1172/JCI26373

Xu M, Lu N, Sun Z et al (2012) Activation of the unfolded protein response contributed to the selective cytotoxicity of oroxylin A in human hepatocellular carcinoma HepG2 cells. Toxicol Lett 212(2):113–125. doi:10.1016/j.toxlet.2012.05.008

Ye SL (2008) Current aspects on standard therapy for primary hepatocellular carcinoma. Zhonghua Gan Zang Bing Za Zhi 16(1):1–2

Yoshida H, Matsui T, Hosokawa N, Kaufman RJ, Nagata K, Mori K (2003) A time-dependent phase shift in the mammalian unfolded protein response. Dev Cell 4(2):265–271

Zinszner H, Kuroda M, Wang X et al (1998) CHOP is implicated in programmed cell death in response to impaired function of the endoplasmic reticulum. Genes Dev 12(7):982–995